

Conversion of 1-Butene to Aromatics over $\text{AlPO}_4\text{-11}$

T. K. BHATIA¹ AND M. J. PHILLIPS²

*Department of Chemical Engineering and Applied Chemistry, University of Toronto,
Toronto, Ontario M5S 1A4, Canada*

Received April 20, 1987; revised October 20, 1987

The activity of the crystalline molecular sieve $\text{AlPO}_4\text{-11}$ for the conversion of 1-butene to benzene, toluene, ethylbenzene, and the xylenes (BTEX) was followed as a function of temperature, time on stream, nickel loading, and methane dilution of the olefin feed. A maximum in liquid production, selectivity to BTEX, and cracking to C(1), C(2), and C(3) products was observed at 773 K. Over 8 h on stream at this temperature, selectivity to benzene and total liquid product increased significantly, the amount of cracked gases increased somewhat, and selectivity to toluene, ethylbenzene, and xylenes decreased somewhat. Nickel loading depressed the amount of BTEX produced probably due to rapid coking of the catalyst. Methane dilution of the feed stream caused a decrease in total liquid product but increased the liquid density as a result of changes in component selectivities. Even in the most favorable case, the activity of $\text{AlPO}_4\text{-11}$ was far less than that of HZSM-5 for the same reaction. The results support a mechanism that proceeds via partial dehydrogenation to butadiene which then participates in a dimerization step, possibly of a Diels-Adler type. C(1) to C(3) products arise from cracking of oligomers and not directly from the 1-butene feed. © 1988 Academic Press, Inc.

INTRODUCTION

The reaction of 1-butene over the crystalline aluminophosphate $\text{AlPO}_4\text{-11}$ was studied as part of ongoing research into olefin oligomerization reactions to give C(6) to C(8) aromatics over molecular sieve catalysts. Liquid product yield and selectivity with respect to benzene, toluene, ethylbenzene, and the xylenes (BTEX) was followed as a function of temperature (673 to 858 K), time on stream, dilution of the olefin feed with methane, and nickel loading of the catalyst.

$\text{AlPO}_4\text{-11}$ was selected because it is an intermediate-pore molecular sieve, its elliptical 10-ring parallel to the *c*-axis having a free crystallographic diameter of 0.67 by 0.40 nm (1, 2). The zeolite ZSM-5, also an intermediate-pore material, is characterized by ellipsoidal 10-ring "straight" chan-

nels with free dimensions approximately 0.54 by 0.56 nm intersected by "sinusoidal" channels with free dimensions 0.51 by 0.54 nm (3). Both materials, therefore, have the potential for shape selectivity. While $\text{AlPO}_4\text{-5}$, $\text{AlPO}_4\text{-11}$, and ZSM-5 have Lewis and Brønsted acid sites, the number, strength, and distribution of the zeolitic acid sites overwhelm those of the aluminophosphates (4-8).

Tabak *et al.* (9) have reported a model reaction path for propylene conversion over ZSM-5 in which the olefin first undergoes oligomerization to a C(6), C(9), or C(12) species which then isomerizes and cracks to a range of light olefins. These, in turn, can copolymerize to heavier isoolefins. The continuous carbon number distribution in the product, independent of the carbon number of the starting olefin, can be explained by this reaction scheme (10).

It was of interest, therefore, not only to follow catalyst activity but also to examine the gaseous and liquid reaction product to determine how well Tabak *et al.*'s model

¹ Present address: U.S. Borax Research Corp., 412 Crescent Way, Anaheim, CA 92801.

² To whom correspondence should be addressed.

reaction path describes the reaction of 1-butene over $\text{AlPO}_4\text{-11}$.

METHODS

The $\text{AlPO}_4\text{-11}$ was prepared as described in Example 32 of U.S. Patent 4,310,440 (10), except that a Pyrex-lined reactor was used rather than a Teflon-lined pressure vessel. In a typical preparation, reagent amounts specified in Example 32 were reduced by a factor of 0.36. Greater success in obtaining a crystalline product resulted when alumina was added to the phosphoric acid and this mixture diluted with water than when alumina was added to a phosphoric acid–water mixture. Small aliquots of catalyst were loaded with nickel by impregnation with 0.013 *M* aq $\text{Ni}(\text{NO}_3)_2$ followed by evaporative drying at room temperature, vacuum drying at 17 kPa and 383–393 K for 5–6 h, and calcination at 773 K in flowing air overnight.

A single batch of $\text{AlPO}_4\text{-11}$ was used for all experiments. This material was characterized by X-ray diffraction (XRD) and the Al/P ratio and Ni loading were determined by inductively coupled argon plasma spectroscopy (ICAP).

Samples of catalyst (0.4 to 0.6 g) were supported between quartz wool plugs held on steel screens at the midpoint of a $\frac{1}{2}$ -in.-o.d. type 316 stainless-steel tubular micro-reactor. The catalyst bed temperature was monitored via a Chromel–Alumel thermocouple inserted into a stainless-steel thermowell. The reactor and tubular preheater ($\frac{3}{16}$ -in.-o.d. stainless-steel) were placed in electric furnaces. Gas lines were $\frac{1}{8}$ -in.-o.d. Teflon connected with Swagelok fittings. Outlet pressures from all gas cylinders were regulated to 200 kPa (15 psig) and gas flow rates (measured by soap bubble flowmeters) were controlled and maintained by a Matheson No. 7352 gas rotameter equipped with No. 610A tubes and a mixing tube.

The product stream was kept at 423 K to prevent in-line condensation between the reactor exit and the condenser system. The 273 K condensate was collected over 2-h

periods in vials which were an integral part of the condenser system. Before analysis, liquid samples were left at room temperature in lightly capped vials overnight because the high volatility of the condensate contributed to unreliable analytical results. (Duplication of this procedure using a gc-calibrated mixture showed an average BTEX loss of only 0.01 g per day.) The density of each liquid sample was determined using either a calibrated 1-ml microflask or a 0.1-ml syringe. The liquid was analyzed on an 18 m \times 0.2-mm-o.d. fused silica thick-film capillary column with a flame ionization detector in a Hewlett–Packard 5790A series gas chromatograph with a 3390A integrator. During the runs, product gas samples were trapped in a 250- μl sampling loop and analyzed on a 1.8 m \times 0.32-cm-o.d. Poropak S 80/100 mesh column with a thermal conductivity detector. Temperature programming (from 313 to 523 K (liquids)) and from 313 to 423 K (gases)) was an integral part of the analysis procedure.

Runs were carried out for 2 or 8 h. A group of 2-h runs performed under the same conditions will be referred to as a set (of experiments). After each set, the reactor was reloaded with fresh catalyst. Prior to a run, the catalyst was treated for 3–5 h in flowing air, the reactor was purged with nitrogen, the reactor temperature was set at 673 K, and hydrogen was passed over the catalyst overnight. (Some pairs of runs, however, were performed on the same day without any pretreatment step in between.) After pretreatment, the reactor was again purged with nitrogen and brought to reaction temperature before the 1-butene feed was introduced.

RESULTS

The Al/P ratio determined by ICAP for the batch of catalyst used in these experiments was 1.04, well within the prescribed tolerance of ± 0.2 (11). Position and intensity of the lines in the XRD pattern of a sample of $\text{AlPO}_4\text{-5}$ supplied by Union Car-

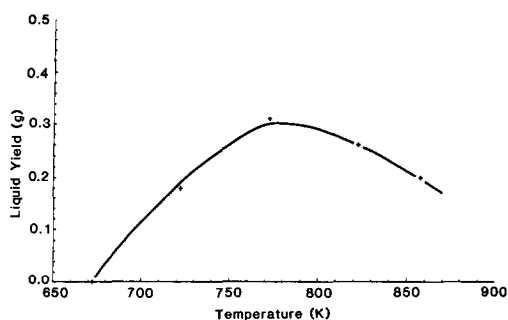


FIG. 1. Liquid yield for a 2-h run versus temperature.

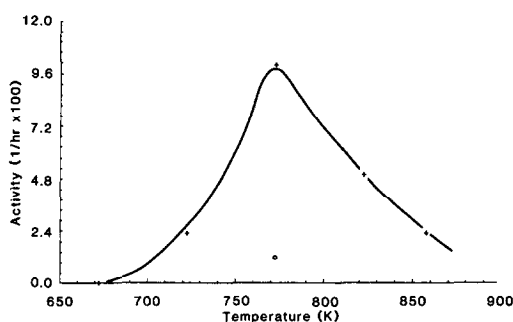


FIG. 3. Activity ($\text{g liquid} \cdot (\text{g catalyst})^{-1} \cdot \text{h}^{-1}$) versus temperature. (+) $\text{AlPO}_4\text{-11}$; (O) glass beads (the blank).

bide were compared with the values listed in the patent (11) in order to calibrate our equipment. The good agreement obtained between line position and intensities of our prepared $\text{AlPO}_4\text{-11}$ sample and the appropriate patent values (9) confirmed the success of our synthesis procedure. The XRD pattern of the 0.425 mass% Ni-loaded $\text{AlPO}_4\text{-11}$ showed no change in crystallinity as a result of the Ni-loading procedure.

The aromatization activity of $\text{AlPO}_4\text{-11}$ was followed as a function of temperature, time on stream, nickel loading, and methane dilution of the olefin feed. Activity is defined as the mass of BTEX per mass of catalyst per hour and calculated as grams liquid per hour times grams BTEX per gram liquid. Selectivity for a component is the mass percent of that component in the liquid. Gas analyses are reported as mass percent of the exit stream. All the components

lighter than the feed are considered here as one unit for convenience and the term "cracked gas" is defined as the sum of the C(1), C(2), and C(3) concentrations in the gaseous product. The product gas analyses did, however, separate paraffin and olefin components through C(4).

Figures 1, 2, 3, and 4 show that, in the temperature range investigated, BTEX selectivity, liquid production, and cracking had maximum values at 773 K. In comparing Figs. 1 and 4, it should be noted that at 673 K, no liquid product was produced so that no BTEX selectivity could be calculated.

The changes in catalyst activity with time at different temperatures are shown in Figs. 5, 6, and 7. Although it appears that cracking values (that is, amounts of "cracked gas" produced) are directly related to activity (the more active systems gave higher

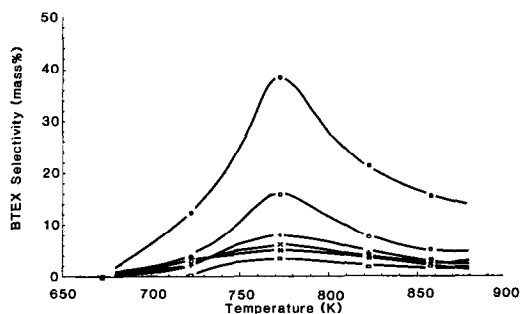


FIG. 2. BTEX selectivity (mass% of liquid product) versus temperature. (●) Total; (○) toluene; (+) benzene; (x) ethylbenzene; (*) *m,p*-xylene; (□) *o*-xylene.

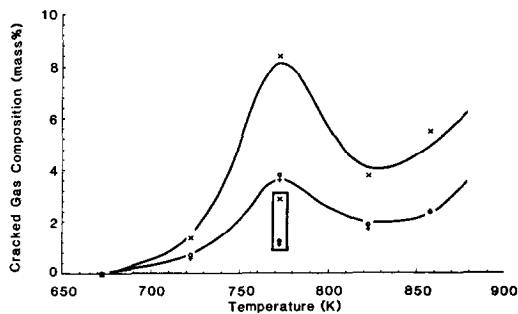


FIG. 4. Cracked gas composition (mass% of total exit gas) versus temperature. (x) C(1); (○) C(2); (□) C(3); values in box were obtained over glassbeads.

TABLE 1

Activity of Nickel-Loaded $\text{AlPO}_4\text{-11}$

Nickel loading ^a (mass%)	Activity ($\text{h}^{-1} \times 10^2$)
None	9.99
0.096	1.55
0.250	2.16
0.334	—
0.425	—

^a As determined by ICAP.

cracking values), the time-dependent changes in activity were not paralleled by changes in cracking. In fact, the cracking values remained essentially constant throughout the 8-h run. However, during the first 1–5 min of many runs, the flow rates of product gases were observed to be much higher than that of the feed gas, indicating that a high degree of cracking occurred in the early stages of these runs.

Nickel Loading

The nickel-loaded catalysts showed much lower activities than did the unloaded. Data are summarized in Table 1. Qualitative examination of catalyst beds after the experiments showed more coking for the nickel-loaded catalyst samples. In fact, the 0.344 and 0.425% nickel catalysts caused so much cracking and coking that reactor plugging occurred within the first

few minutes of the run, effectively stopping the experiment. When these two catalyst samples were removed from the reactor, it was observed that the particles had become bound together with a carbon matrix into a pellet.

Methane as Diluent

Addition of methane to the 1-butene feed stream decreased activity and liquid yield but increased the density of the liquid product. Selectivities to the lighter aromatic components (benzene and toluene) were reduced while selectivities to the heavier aromatic components were enhanced. Data are given in Table 2. Runs having the same number (for example, 48 and 48A) were performed in a single day without a regeneration step in between. In order to discount any time-on-stream effects, runs with methane and without methane were duplicated but in reverse order.

Catalyst Crystallinity

In Table 3, results with samples from two different batches of $\text{AlPO}_4\text{-11}$ are compared with those from a comparable experiment in which the reactor was loaded with glass beads. $\text{AlPO}_4\text{-11}$ [1] is a sample from the batch used in all of the work reported in this paper. $\text{AlPO}_4\text{-11}$ [2] is a sample from a batch judged to be less crystalline because of line broadening observed in the XRD spectrum.

TABLE 2

Methane Addition to 1-Butene Feed

Run	Temp. (K)	1-C ₄ H ₈ flow ($\text{g} \cdot \text{h}^{-1}$)	1-C ₄ H ₈ / CH ₄ ($\text{mol} \cdot \text{mol}^{-1}$)	Liquid			Liquid selectivity ^a					Activity ($\text{h}^{-1} \times 10^2$)	
				Mass (g)	Dens. ($\text{g} \cdot \text{ml}^{-1}$)	Yield (mass%)	Benzene	Toluene	Ethyl- benzene	<i>m,p</i> - xylene	<i>o</i> - xylene		Total BTEX
48	773	5.9	2.1	0.164	0.81	1.4	4.1	7.1	4.6	4.5	1.9	22.2	3.7
48A	773	5.9	—	0.738	0.78	6.2	6.4	6.8	1.8	0.97	0.61	16.6	12.2
49	773	6.2	—	0.335	0.80	2.7	8.2	16.4	5.9	4.5	2.8	37.8	12.8
49A	773	6.2	2.2	0.181	0.83	1.5	3.8	10.6	6.0	4.7	2.8	27.9	5.1
64	823	6.1	2.9	0.065	0.81	0.53	1.8	6.2	6.9	7.6	4.4	26.9	1.8
64A	823	6.1	—	0.210	0.81	1.7	5.0	8.9	4.8	4.3	2.4	25.4	5.4
65	823	6.3	—	0.101	0.84	0.80	3.2	15.7	7.3	5.7	5.1	37.0	3.7
65A	823	6.3	3.0	0.062	0.84	0.49	—	3.5	8.9	5.9	5.7	24.0	1.5

^a All values are given as mass percent of total liquid.

TABLE 3
 Reaction of 1-Butene at 773 K

Catalyst	Gas flow (g · h ⁻¹)	Liq. prod. (g)	Liquid selectivity ^a					Activity (h ⁻¹) × 10 ²	Cracked ^b gases
			Benzene	Toluene	Ethyl- benzene	Xylenes	Total BTEX		
AlPO ₄ -11 [1]	6.2	0.314	7.9	16.0	6.2	8.5	38.6	10.0	15.8
AlPO ₄ -11 [2]	6.4	0.132	2.4	7.2	5.0	7.6	22.2	2.8	2.5
Glass beads	5.9	0.056	1.5	7.6	6.5	8.0	23.6	1.2	5.2

^a Mass percent of total liquid mass.

^b Mass percent of (C₁ + C₂ + C₃) in the exit gas stream.

DISCUSSION

The maximum in activity and selectivity to aromatics observed for AlPO₄-11 at 773 K is in sharp contrast with literature data for ZSM-5 which indicate much higher activity at lower temperatures (12–14). The low aromatization activity of AlPO₄-11 is more likely to be a consequence of the nature and strength of its acidity rather than of pore shape and size.

The aromatic products in this study were restricted to carbon numbers of 8 or less. Analysis by gas chromatography did not show peaks in the propylbenzene or butylbenzene ranges. Over ZSM-5, however, the product has a cutoff point at 10 carbons (12). Reactions catalyzed by ZSM-5 are thought to involve carbenium ion mechanisms and products are restricted in size by channel geometries. Since the channel dimensions of the ZSM-5 and the AlPO₄-11 are similar, but the carbon number cutoff points of the products are different, it is reasonable to postulate that the reactions catalyzed by AlPO₄-11 do not involve carbenium ions as intermediates. The involvement of units smaller than C(4) in the oligomerization process would likely have resulted in the formation of 9- and 10-carbon aromatics. It has been brought to our attention that the >C₈ aromatic products which form in ZSM-5 may form at channel intersections and are therefore not present in the AlPO₄-11 product due to a transition

state selectivity which the one-dimensional AlPO₄-11 possesses but which the two-dimensional ZSM-5 lacks. The channel dimensions in AlPO₄-11 preclude the formation of trimers and large polymers of 1-butene. Hence, reactions such as cracking to produce smaller units and dehydrogenation/cyclization to produce aromatics likely involve dimer units of the 1-butene feed.

Possible pathways for the dimerization of two C(4) units are by polarization of adsorbed olefins on Lewis sites (15), or by a Diels–Alder mechanism, which is also catalyzed by Lewis sites (16). In a Diels–Alder reaction, a diolefin contributes four carbons while an olefin (or another diolefin) contributes two carbons to the six-membered ring of a cyclic compound. Aromatics can then be produced by dehydrogenating the cyclic compounds. Metal oxides and phosphates are known to catalyze the dehydrogenation of monoolefins to diolefins (16, 17). Analysis of the gaseous product in our work showed a consistent production of 1,3-butadiene. For example, at 823 K, the amount of 1,3-butadiene in the product gases was 46% of that percentage of methane. Aitken (18) has shown that 1,3-butadiene can react over nickel-treated amorphous aluminum phosphate, most probably by a Diels–Alder cycloaddition, to produce 4-ethenylcyclohexene with a high selectivity.

Further evidence to support the dimerization process and to discount the carbe-

nium ion mechanism can be obtained from analysis of the gaseous product. The BTEX activity is seen to vary directly with the cracking rate. At 673 K, no liquid products and very little cracking were detected. At 773 K, maxima for activity, liquid production, and cracking values were observed. Beyond 773 K, the value of all three decreased. This indicates that the C(1) to C(3) molecules are not primary products from the direct cracking of the 1-butene feed (as would be the case for the carbenium ion mechanism) but, rather, are secondary products from the cracking of 1-butene oligomers (19–21). However, some thermal cracking of the feed occurs at higher temperatures; at 858 K, the cracking rate is higher than that at 723 K, but the activities and liquid productions are nearly equal.

The drop in activity for temperatures above 773 K cannot be explained entirely by higher cracking rates. Such an explanation would require the cracking rate to increase continuously with temperature and could not explain the observed cracking maximum. Clearly, some other phenomenon must also play a role in the process and oppose the temperature-related increases in oligomerization and cracking activities. One explanation may be that reactant transport in the intracrystalline pores was increasingly hindered at higher temperatures by pore mouth blocking. This theory was offered by van den Berg *et al.* (22) who, in their study of the reactions of small olefins over HZSM-5, observed less effective filling of the pore volume by oligomers formed at higher temperatures (in this case, over 300 K).

Examination of the best liquid yield case (at 773 K) shows that the (molar) yield for the cracked gas was more than 15 times greater than that for the sum of the aromatics. (Other runs had even higher cracked gas to aromatics ratios.) This would indicate that only a small fraction of the oligomers formed was converted to aromatics and that most of the oligomers were cracked. It is important to keep in mind

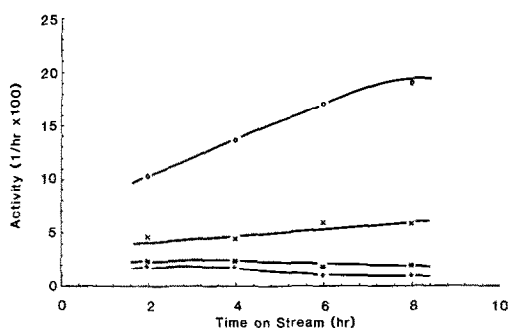


Fig. 5. Activity ($\text{g liquid} \cdot (\text{g catalyst})^{-1} \cdot \text{h}^{-1}$) versus time on stream. (○) 773 K; (×) 823 K; (*) 858 K; (+) 723 K.

that, in the best case, when ~40 mass% of liquid consists of aromatics, ~60 mass% consists of C(6)+ aliphatics. (Any C(5) formed would evaporate overnight before analysis.) This aliphatic fraction is larger at lower and higher temperatures. In fact, at 723 K, the C(6)+ aliphatics make up more than 90 mass% of the liquid product. It would appear, therefore, that the cyclization/dehydrogenation step is rate limiting in aromatics production over $\text{AlPO}_4\text{-11}$.

Time-dependent changes in activity at 773 K were not paralleled by changes in cracking. The constancy of cracking values, though, is not inconsistent with the proposed theory which relates cracking and activity. Systems that have high activity will produce large quantities of oligomers and will also have high cracking values. The relative positions of the curves in Figs. 5 and 7 are consistent with this argument. It

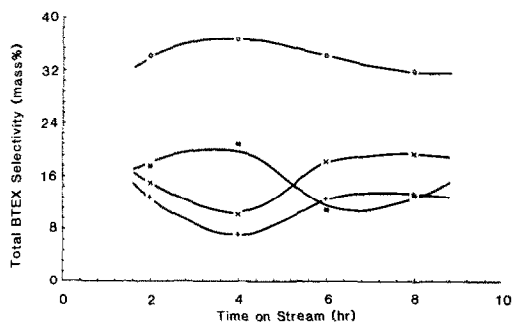


Fig. 6. Total BTEX selectivity (mass percent of liquid product) versus time on stream. (○) 773 K; (*) 858 K; (×) 823 K; (+) 723 K.

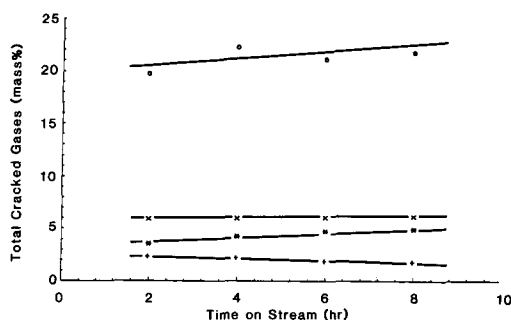


FIG. 7. Total cracked gas (mass% of C(1) + C(2) + C(3) in exit gas) versus time on stream. (O) 773 K; (x) 823 K; (*) 858 K; (+) 723 K.

is well known that, with zeolites, cracking reactions and olefin oligomerization activity increase with Brønsted acid site density (23). In the case of the crystalline aluminophosphates, the differences in electronegativities between Al(1.61) and P(2.19) will set up electron withdrawing dipole moments which are able to polarize the double bonds of adsorbed olefins and, thus, can be regarded as Lewis acid sites. Wilson *et al.* (2) and Bond and co-workers (24) report a ν_{OH} absorption at 3680 cm^{-1} for several $AlPO_4$'s which has been attributed (25) to $\nu_{(P-OH)}$. Ji and Xu (7) have recently published the TPD spectrum for *n*-butylamine on $AlPO_4-11$ in which only two peaks are seen, one at $\sim 373\text{ K}$ associated with physical adsorption and a larger peak at $\sim 640\text{ K}$ associated with weak chemisorption. (With their Ni-loaded $AlPO_4-11$, both before and after reduction in H_2 at 773 K, they observed a decrease in physical adsorption and an increase in amount and type of chemisorbed amine.) Choudhary and Akolekar (5) from their more extensive studies of pyridine chemisorption concluded that $AlPO_4-5$ possesses both Lewis and Brønsted acid sites but that only a very few are strong acid sites, the majority of sites being weaker ones. They also cite their unpublished data to the effect that, in terms of pyridine chemisorption at 623 K, $AlPO_4-5$'s strong acid sites are only 2.2% of HZSM-5's total (for a zeolite with Si/Al =

17.2, in terms of $\text{mmol} \cdot \text{g}^{-1}$). If we make the inference that the chemically similar $AlPO_4-11$ also possesses weak Lewis and Brønsted sites, our experimental observation that only a small fraction of the oligomers formed is converted to aromatics is reasonable in that cracking and dimerization will require weaker acid sites (of which there are relatively many) than will dehydrocyclization (for which there are relatively few). Therefore, time-dependent increases in activity may result in higher yields for aromatics but will affect the cracking values only marginally. Choudhary and Akolekar (5) associated the rapid decrease in $AlPO_4-5$ activity for cumene cracking and methanol conversion to coke deposition at channel openings. On the other hand, they also attributed the increase in activity with time (that is, with pulse number) for isooctane cracking and aromatics yield in ethanol conversion to catalytically active sites on the coke. The maximum they observed in the conversion with time of *n*-hexane, toluene, and *o*-xylene, also attributed to active sites on carbon, was not observed by us but the increase in activity with time that we observed at 723 K (Fig. 6) may well be due to catalytic sites on coke.

The low activities of the nickel-loaded catalysts can be attributed to rapid deactivation of the catalyst by coking. The coke buildup was so rapid and severe, that, for the catalysts with the higher nickel loadings, reactor plugging occurred within the first few minutes of the run. The activity of nickel for hydrogenation/dehydrogenation has led to its use at high temperatures and in hydrogen-poor environments, for hydrogen abstraction. While the dehydrogenation of cyclic oligomers may produce aromatics, excessive dehydrogenation will lead to the formation of coke deposits.

Methane was mixed into the feed without decreasing the flow of 1-butene. Hence, methane addition simultaneously diluted the feed and increased the gas velocity. The lower liquid yields and activities for the 1-

butene plus methane feeds may have been caused by dilution effects, lower contact times, or a combination of the two.

The changes in liquid densities and selectivities that arose from the addition of methane provide supplemental evidence to support the dimerization-cracking argument. Increased gas velocities resulted in decreased contact times and increased concentrations of 8-carbon aromatics (ethylbenzene and xylenes) at the expense of the concentrations of the lighter aromatics (benzene and toluene). Also, the liquid densities were greater for the higher flow rate cases. These results suggest that the larger and denser molecules were produced first and that the smaller aromatics were produced from the cracking (dealkylation) of the larger aromatics.

With regard to crystallinity, the more crystalline $\text{AlPO}_4\text{-11}$ [1], as expected, produced more aromatics than did the less crystalline $\text{AlPO}_4\text{-11}$ [2], showing that crystal structure and, thus, shape selectivity play an important role. Also, the less crystalline material produced less cracked gases further supporting the contention that the C(1) to C(3) components were not produced directly from the feed but from oligomers.

In conclusion, the product distribution and the effect of the catalyst crystallinity on activity are a result of shape selectivity. The aromatization process over $\text{AlPO}_4\text{-11}$ appears to proceed via an initial partial dehydrogenation to a diene which then participates in the dimerization step, possibly of a Diels-Alder type. Molecules in the C(1) to C(3) range are not produced directly from the 1-butene feed but from the cracking of oligomers. Thus, the reaction model of Tabak *et al.* (9) does describe the processes occurring over $\text{AlPO}_4\text{-11}$ if the essential preliminary formation of diene is included in the path. The addition of nickel to the catalyst depressed BTEX production probably because of rapid deactivation of the catalyst by coke.

ACKNOWLEDGMENTS

The authors express their gratitude to Dr. E. M. Flanigen of Union Carbide Corp. for supplying a research sample of $\text{AlPO}_4\text{-5}$. The helpful comments and suggestions of Mr. G. W. Norval and his invaluable assistance in the preparation of this manuscript are gratefully acknowledged. Financial support for this work was provided by the Natural Sciences and Engineering Research Council of Canada.

REFERENCES

1. Bennett, J. M., and Smith, J. V., *Z. Kristallogr.* **171**, 65 (1985).
2. Wilson, S. T., Lok, B. M., Messina, C. A., Cannan, T. R., and Flanigen, E. M., *J. Amer. Chem. Soc.* **104**, 1146 (1982); Wilson, S. T., Lok, B. M., Messina, C. A., Cannan, T. R., and Flanigen, E. M., *ACS Symp. Ser.* **218**, 79 (1983).
3. Olson, D. H., Kokotailo, G. T., Lawton, S. L., and Meier, W. M., *J. Phys. Chem.* **85**, 2238 (1981).
4. Vedrine, J. C., Auroux, A., Bolis, V., Dejaifve, P., Naccache, C., Wierzchowski, P., Derouane, E. G., Nagy, J. B., Gilson, J-P., van Hooff, J. H. C., van den Berg, J. P., and Wolthuizen, J., *J. Catal.* **59**, 248 (1979); Auroux, A., Bolis, V., Wierzchowski, P., Gravelle, P., and Vedrine, J. C., *J. Chem. Soc. Faraday Trans. 1* **75**, 2544 (1979).
5. Choudhary, V. R., and Akolekar, D. B., *J. Catal.* **103**, 115 (1987).
6. Choudhary, V. R., and Nayak, V. S., *Zeolites* **5**, 15 (1985).
7. Ji, M., and Xu, Q-h., *Cuihua Xuebao (J. Catal., Dalian)* **8**, 41 (1987).
8. Dworezkov, G., Rimplmayr, G., Mayer, H., and Lercher, J. A., in "Adsorption and Catalysis on Oxide Surfaces" (M. Che and G. C. Bond, Eds.), p. 163. Elsevier, Amsterdam/New York, 1985.
9. Tabak, S. A., Krambeck, F. J., and Garwood, W. E., *AIChE J.* **32**, 1526 (1986).
10. Garwood, W. E., *Prepr. Div. Pet. Chem. Amer. Chem. Soc.* **27**(2), 563 (1982); Garwood, W. E., *ACS Symp. Ser.* **218**, 383 (1983).
11. Wilson, S. T., Lok, B. M., and Flanigen, E. M., U.S. Patent 4,310,440 (1982).
12. Chang, C. D., *Catal. Rev. Sci. Eng.* **25**, 1 (1983).
13. Virk, K. S., M.A.Sc. thesis, Department of Chemical Engineering and Applied Chemistry, University of Toronto, 1985.
14. Norval, G. W., and Phillips, M. J., unpublished results.
15. Beran, S., Jiru, P., and Kubelkova, L., *J. Mol. Catal.* **16**, 299 (1982).
16. Langner, B. E., and Meyer, S., in "Proceedings of the International Symposium on Catalyst Deactivation, Antwerp, Oct. 13-15, 1980." Elsevier, Amsterdam, New York.

17. Moffat, J. B., *Catal. Rev. Sci. Eng.* **18**, 199 (1978).
18. Aitken, D. M., B.A.Sc. thesis, Department of Chemical Engineering and Applied Chemistry, University of Toronto, 1985.
19. Abbot, J., and Wojciechowski, B. W., *Canad. J. Chem. Eng.* **63**, 818 (1985).
20. Abbot, J., and Wojciechowski, B. W., *Canad. J. Chem. Eng.* **63**, 278 (1985).
21. Abbot, J., Cormac, A., and Wojciechowski, B. W., *J. Catal.* **92**, 398 (1985).
22. van den Berg, J. P., Wolthuisen, J. P., and van Hooff, J. H. C., *J. Catal.* **80**, 139 (1983).
23. Shihabi, D. S., Garwood, W. E., Chu, P., Miale, J. N., Lago, R. M., Chu, C. T-W., and Chang, C. D., *J. Catal.* **93**, 471 (1985).
24. Bond, G. C., Gelsthorpe, M. R., Sing, K. S. W., and Theocharis, C. R., *J. Chem. Soc. Chem. Commun.* **15**, 1056 (1985).
25. Peri, J. B., *Discuss. Faraday Soc.* **52**, 55 (1971).